Computing Applied Force Constraints for Insertion Tasks Using Halfspace Intersection Projections [1]

Gordon Dakin
Robin Popplestone

COINS Technical Report 90-56
July 9, 1990

Laboratory for Perceptual Robotics
Department of Computer and Information Science
A305, Graduate Research Center
University of Massachusetts
Amherst, MA 01003

[1] Preparation of this paper was supported by grant number N00014-86-K-0764 from the Office of Naval Research.

Abstract

An algorithm is presented for projecting the intersection of m linear halfspaces from $\Re^n$ into a lower-dimensional subspace of $\Re^n$. The algorithm serves as a computational tool in the planning of compliant motions for insertion tasks. In the point-contact states of an insertion task, the 6 forces and torques applied by a robot to an insertor entering a container relate quasi-statically to the reaction forces at some n points of contact between the insertor and container via a $6 \times 3n$ matrix. Prohibition of failure modes such as jamming or excess contact strain can be expressed through linear inequalities over the reaction forces. These constraints restrict the contact force combinations to halfspaces in $\Re^{3n}$. Viewing the $6 \times 3n$ matrix as a projection map from $\Re^{3n}$ to $\Re^6$, the halfspace intersection volume can be projected into applied wrench space to yield an intersection of $\Re^6$-halfspaces from which a command wrench may be selected. Our projection method effectively automates and extends to 3 dimensions the manual force constraint derivation approach of Whitney [11]. However, we prove that if the applied wrench space is of lower dimension than the space of contact force components, as is the case in Whitney's derivation, the resulting applied wrench constraints provide only necessary, not sufficient, conditions for avoiding failure modes such as jamming.

1 Introduction

The automation of industrial assembly operations such as peg-in-hole insertions calls for the automatic planning of compliant motions. In one approach to compliant motion planning, a nominal trajectory is first computed, for the *moving part* to follow relative to the *stationary part*. Possible states of contact between the two parts are then anticipated, given the uncertainty in the moving part's trajectory and the parts' geometries. A compliant control strategy is then selected to accommodate the anticipated contact states by attempting to circumvent failure modes such as jamming, wedging, deformation of parts, or simply failure to achieve the goal configuration.

These failure modes are largely dependent on the direction and magnitude of the reaction forces occuring at the parts' contacting features. For instance, jamming (static friction) can be avoided by preventing the reaction forces from entering the friction cones of the contacting surfaces. Movement toward the goal configuration can also be guaranteed by imposing desired directions on the sliding frictional forces. Once inequality constraints are established over the contact forces, one may derive a corresponding set of constraints over the wrench (force and torque) which the robot exerts through the moving part's coordinate frame. As demonstrated in section 2 and proven in section 4, however, these wrench constraints may only provide necessary, not sufficient, conditions for satisfying the constraints imposed on the contact forces.

A derivation of reaction force constraints, and in turn, applied force constraints for jamming avoidance was first performed by Simunovic [10], and later by Whitney [11]. These authors analyzed the 2-dimensional peg-in-hole problem (see figure 1) using the assumption that the peg behaved quasi-statically, without the influence of inertial forces. Whitney used this simplified relationship between the contact forces and applied wrench to derive applied wrench constraints for jamming avoidance in the 1-point and

2-point contact states of the peg-in-hole task. Although widely regarded as sufficient conditions for jamming avoidance, the applied wrench constraints derived by Whitney for the 2-point contact state are, in fact, only necessary conditions (see section 2).

Force analysis of the peg-in-hole problem has been extended to multiple insertion tasks [6] and to 3-dimensional parts [1][7]. Caine [1] introduced the *breaking-contact* constraint on contact forces, which guarantees that the contacting surfaces will not separate. This constraint is useful for enforcing a desired sequence of contact states in which the number of contacts increases progressively throughout the trajectory. As demonstrated in [2], such a strategy is sometimes necessary if an applied force satisfying all anticipated contact states is to be found. Adopting a designer approach to compliant motion planning in 3 dimensions, Caine [1] developed tools for computing and visualizing nonlinear jamming-avoidance and breaking-contact constraints over the 6-dimensional applied force.

The techniques outlined above are sometimes referred to as the "manual methods" of compliant motion planning. Their major drawback is that the applied force constraint derivations are tedious and time-consuming, especially in 3 dimensions. This report offers a tool for performing these derivations automatically. In section 2, Whitney's derivation of applied wrench constraints for jamming avoidance in the 2-point contact state is recast as a projection of the intersection of two contact force halfspaces from $\Re^4$ into 3-dimensional applied force space. We also demonstrate that the resulting applied wrench constraints cannot guarantee that jamming will not occur at one of the two contacts. Section 3 presents a general algorithm for projecting an intersecton of halfspaces in $\Re^n$ into a lower-dimensional space. In section 4, we prove that constraints thus derived only guarantee that at least one of the higher-dimensional constraints will be satisfied.

Section 5 describes how this algorithm may be used as a tool for deriv-

ing applied wrench constraints from local constraints imposed on the contact forces involved in 3-dimensional insertion tasks. Linear contact force constraints are established for avoiding the error modes of part deformation, breaking of contact, and jamming. The contact force constraints are then projected into applied wrench space, yielding a set of linear constraints on the applied forces and torques which serve as necessary conditions for avoiding the error modes. Finally, section 6 discusses how to incorporate our projection method into the synthesis of compliant control strategies.

2 Whitney's technique recast as a projection

The 2-dimensional peg-in-hole problem, as analyzed by Simunovic [10] and later by Whitney [11], calls for the derivation of an *applied wrench*, to be exerted through the peg coordinate frame, that will not result in *jamming*, i.e., static friction, at the contact sites. In the *2-point contact* state (see figure 1), the jamming avoidance requirement amounts to ensuring that the contact forces $\mathbf{f}_1$ and $\mathbf{f}_2$ lie outside of the friction cones associated with the contacting surfaces. Representing the friction cones as a pair of equations relating the normal and lateral components of each contact force, Whitney manually derives a linear inequality constraint in 3-dimensional applied force space. These applied wrench constraints are widely regarded as sufficient conditions for preventing jamming at either of the two contacts. As we show at the end of this section, however, jamming may still occur at a single contact, even if these constraints are satisfied.

With a view towards automating the process of deriving applied force constraints to serve as necessary conditions for the avoidance of jamming and other failure modes, the manual approach of Whitney is reconfigured here as the projection of a 4-dimensional contact force constraint region into 3-dimensional applied force space.

Figure 1 illustrates a rectangular peg of radius r, inserted into a rect-

angular hole to a depth of L and with an orientation of θ. A hole vertex exerts a force $\mathbf{f}_1$ against a peg wall, while a hole wall exerts a force $\mathbf{f}_2$ against a peg vertex. If $\mid \theta \mid$ is small, the jamming avoidance requirement may be expressed as the pair of inequalities $\mu f_{1x} \leq f_{1y}$, $-\mu f_{2x} \leq f_{2y}$, where μ is the coefficient of friction. These constraints not only forbid jamming, but also require the peg to slide in the right direction.

Adopting Whitney's quasi-static assumption, the three applied wrench components (forces F_x, F_y and moment M) relate to the contact forces as follows:

$$\begin{pmatrix} F_x \\ F_y \\ M \end{pmatrix} = \begin{pmatrix} -1 & 0 & -1 & 0 \\ 0 & -1 & 0 & -1 \\ L & r & 0 & -r \end{pmatrix} \begin{pmatrix} f_{1x} \\ f_{1y} \\ f_{2x} \\ f_{2y} \end{pmatrix} \tag{1}$$

The jamming avoidance constraints may be reformatted as inequalities in $\mathbf{f}_1 \times \mathbf{f}_2$ space, to conform with equation (1)'s 4-dimensional respresentation of contact force combinations:

$$\mu f_{1x} - f_{1y} + 0 f_{2x} + 0 f_{2y} \leq 0 \tag{2}$$

$$0 f_{1x} + 0 f_{1y} - \mu f_{2x} - f_{2y} \leq 0 \tag{3}$$

This pair of contact force constraints defines the intersection of two halfspaces in 4-dimensional contact force space. We now wish to characterize the set of applied forces $(F_x F_y M)^T$ that are associated with this contact force halfspace intersection through the quasi-static equation (1).

The 3×4 matrix A in equation (1) may be regarded as a projection map from $\Re^4$ into $\Re^3$. Accordingly, the set of applied forces in $\Re^3$ comprising the A-projected contact force volume must be represented by a set of inequalities in $\Re^3$. Each inequality corresponds to an $\Re^3$-halfspace bounded by a

2-dimensional surface. Any 2-dimensional surface bounding the intersection volume's projection into 3-dimensional applied force space must be the projection of one of the volume's 2-dimensional surfaces. Therefore, in order to obtain inequality descriptions of the projected constraint region in applied force space, we must first compute descriptions of the 2-dimensional surfaces bordering the contact force constraint region, and then project those surfaces into applied force space.

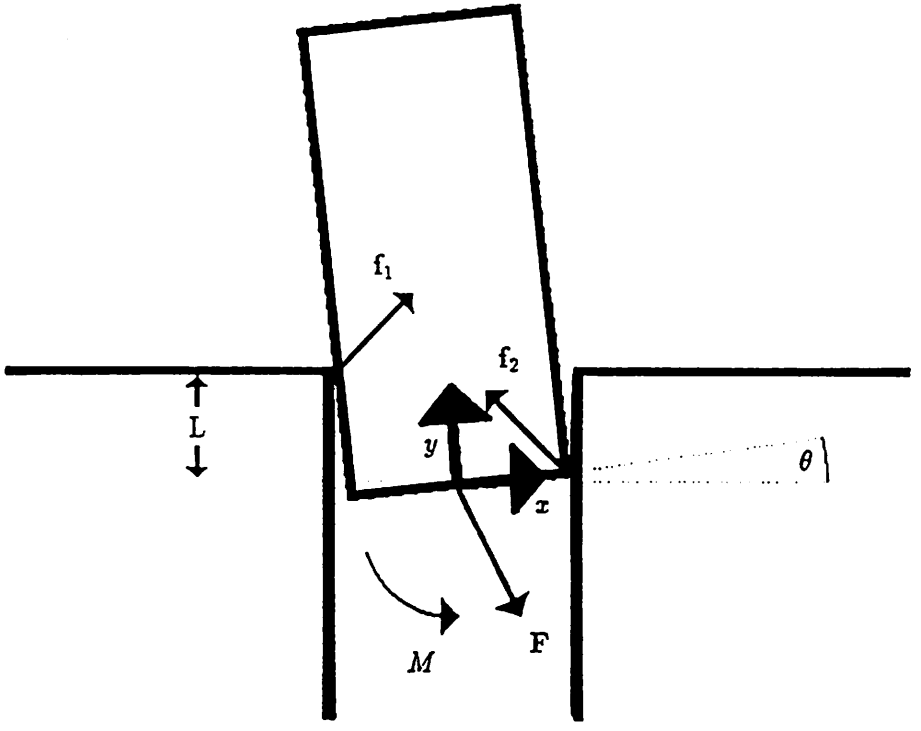

Figure 1. 2-point contact state of the 2-D peg-in-hole operation

The volume in $\Re^4$ defined by the intersection of contact force halfspaces is bounded by two 3-dimensional surfaces, whose outward-pointing normals are just the left-hand-sides of the contact force inequalties (2) and (3):

$$\mathbf{n}_1 = \begin{pmatrix} \mu \\ -1 \\ 0 \\ 0 \end{pmatrix}, \mathbf{n}_2 = \begin{pmatrix} 0 \\ 0 \\ -\mu \\ -1 \end{pmatrix}$$

The two constraint surfaces in $\Re^4$ intersect to form a 2-dimensional surface S of the contact force constraint volume. A basis for the vector space which comprises S consists of any two independent vectors $\mathbf{u}_1$ and $\mathbf{u}_2$ that are orthogonal to both $\mathbf{n}_1$ and $\mathbf{n}_2$. For example,

$$\mathbf{u}_1 = \begin{pmatrix} 1 \\ \mu \\ 0 \\ 0 \end{pmatrix} \quad \mathbf{u}_2 = \begin{pmatrix} 0 \\ 0 \\ -1 \\ \mu \end{pmatrix}$$

The projection S' of S into applied force space is obtained by projecting the basis vectors $\mathbf{u}_1$ and $\mathbf{u}_2$ of S to yield a basis $\{\mathbf{u}'_1, \mathbf{u}'_2\}$ for S'.

$$\mathbf{u}'_1 = A\,\mathbf{u}_1 = \begin{pmatrix} -1 & 0 & -1 & 0 \\ 0 & -1 & 0 & -1 \\ L & r & 0 & -r \end{pmatrix} \begin{pmatrix} 1 \\ \mu \\ 0 \\ 0 \end{pmatrix} = \begin{pmatrix} -1 \\ -\mu \\ L + \mu r \end{pmatrix}$$

$$\mathbf{u}'_2 = A\,\mathbf{u}_2 = \begin{pmatrix} -1 & 0 & -1 & 0 \\ 0 & -1 & 0 & -1 \\ L & r & 0 & -r \end{pmatrix} \begin{pmatrix} 0 \\ 0 \\ -1 \\ \mu \end{pmatrix} = \begin{pmatrix} 1 \\ -\mu \\ -\mu r \end{pmatrix}$$

We finally compute the surface normal of S' as the vector orthogonal to its surface tangents $\mathbf{u}'_1$ and $\mathbf{u}'_2$:

$$\mathbf{n} = \mathbf{u}_1' \times \mathbf{u}_2' = \begin{pmatrix} -1 \\ -\mu \\ L + \mu r \end{pmatrix} \times \begin{pmatrix} 1 \\ -\mu \\ -\mu r \end{pmatrix} = \begin{pmatrix} 2\mu^2 r + \mu L \\ L \\ 2\mu \end{pmatrix}$$

Noting that S' passes through the origin, its surface normal $\mathbf{n}$ gives rise to an applied force inequality which agrees with the result of Whitney [54.5] [2]:

$$(2\mu^2 r + \mu L)F_x + LF_y + 2\mu M \leq 0$$

As we will prove in the section 4, constraint inequalities derived in a lower-dimensional space from a set of inequalities in a higher-dimensional space do not guarantee the satisfaction of the higher-dimensional constraints. The applied wrench constraint derived above is no exception. To demonstrate that this constraint does not always prevent jamming at one of the two contacts, let $\mu = 0.25$ and $L = r = 1$. The jamming constraints on the reaction forces become $\frac{f_{1x}}{4} \leq f_{1y}$, $-\frac{f_{2x}}{4} \leq f_{2y}$, and the above applied wrench constraint becomes

$$\frac{3}{8} F_x + F_y + \frac{1}{2} M \leq 0$$

Let us choose reaction forces

$$\mathbf{f}_1 = \begin{pmatrix} 3 \\ 0 \end{pmatrix}, \mathbf{f}_2 = \begin{pmatrix} -1 \\ 1 \end{pmatrix}$$

Observe that the constraint on $\mathbf{f}_2$, but not the constraint on $\mathbf{f}_1$, is satisfied. We now calculate the applied wrench via equation 1:

[2] We have used F_y where Whitney used $-F_x$.

$$\begin{pmatrix} F_x \\ F_y \\ M \end{pmatrix} = \begin{pmatrix} -1 & 0 & -1 & 0 \\ 0 & -1 & 0 & -1 \\ 1 & 1 & 0 & -1 \end{pmatrix} \begin{pmatrix} 3 \\ 0 \\ -1 \\ 1 \end{pmatrix} = \begin{pmatrix} -2 \\ -1 \\ 2 \end{pmatrix}$$

This wrench satisfies the applied wrench constraint, but as we have seen, it can give rise to a combination of contact forces causing one of the contacts to jam.

3 Halfspace intersection projections

In this section we develop a means for computing the projection of an intersection of halfspaces from $\Re^{n_1}$ to $\Re^{n_2}$, where $n_1 > n_2$. Given a description of m_1 hyperplanar halfspaces in $\Re^{n_1}$ and an $n_2 \times n_1$ projection matrix A ($n_2 \leq n_1$), we wish to describe the set of points $\mathbf{q} \in \Re^{n_2}$ that are images of any point $\mathbf{p} \in \Re^{n_1}$ residing in the m_1 halfspaces' intersection. In particular, we wish to recover the projection of the m_1 halfspaces' intersection as the intersection of some m_2 halfspaces in $\Re^{n_2}$.

Let us denote the m_1 halfspaces in $\Re^{n_1}$ by $\Gamma_1(\mathbf{n}_1, d_1), \ldots, \Gamma_{m_1}(\mathbf{n}_{m_1}, d_{m_1})$, with $\mathbf{n}_i \in \Re^{n_1}$ and $d_i \in \Re$, such that a point $\mathbf{x} \in \Re^{n_1}$ is in halfspace $\Gamma_i(\mathbf{n}_i, d_i)$ iff $\mathbf{n}_i \cdot \mathbf{x} \leq d_i$. The halfspace intersection volume in $\Re^{n_1}$ is bounded by up to m_1 hyperplanes of dimension $(n_1 - 1)$. Similarly, the projected volume in $\Re^{n_2}$ is bounded by some m_2 hyperplanes of dimension $n_2 - 1$. Each of the latter $(n_2 - 1)$-dimensional hyperplanes is the projection of at least one $(n_2 - 1)$-dimensional facet bounding the intersection volume in $\Re^{n_1}$. Note that not every $(n_2 - 1)$-dimensional facet of the intersection volume in $\Re^{n_1}$ necessarily projects to a bordering facet of the projected volume in $\Re^{n_2}$.

The task of recovering the projected volume's description therefore entails (1) computing the $(n_2 - 1)$-dimensional facets of the original volume in

$\Re^{n_1}$ (2) computing those facets' A-projections into $\Re^{n_2}$, and (3) determining which of those facets' projections border the projected volume.

(1) and (2) are fairly straightforward. Let $k = n_1 - n_2 + 1$. The hyperplanes associated with a k-tuple of halfspaces $\Gamma_1(\mathbf{n}_1, d_1), \ldots, \Gamma_k(\mathbf{n}_k, d_k)$ in $\Re^{n_1}$ intersect at an $n_2 - 1$-dimensional facet S if the hyperplane normals $\mathbf{n}_1, \ldots, \mathbf{n}_k$ are independent. The Gram-Schmidt process can then be employed to calculate $n_2 - 1$ surface tangents $\mathbf{u}_1, \ldots \mathbf{u}_{n_2-1} \perp \mathbf{n}_1, \ldots, \mathbf{n}_k$ which span the affine space comprising the $(n_2 - 1)$-dimensional facet. A sample point $\mathbf{p}$ in the affine space may be found by solving n_1 simultaneous equations $\mathbf{n}_i \cdot \mathbf{p} = d_i, i = 1, \ldots, k,\ \mathbf{u}_i \cdot \mathbf{p} = 0, i = 1, \ldots, n_2 - 1$. Thus the facet's affine space S consists of the set

$$S = \{\mathbf{x} \in \Re^{n_1} \mid \mathbf{x} = \mathbf{p} + \sum_{i=1}^{n_2-1} b_i \mathbf{u}_i,\ b_i \in \Re\}$$

The affine space S' comprising the projection of S by A into $\Re^{n_2}$ consists of

$$S' = \{\mathbf{x}' \in \Re^{n_2} \mid \mathbf{x}' = A\mathbf{p} + \sum_{i=1}^{n_2-1} b_i A\mathbf{u}_i, b_i \in \Re\}$$

If the $n_2 - 1$ basis vectors $A\mathbf{u}_1, \ldots, A\mathbf{u}_{n_2-1}$ in $\Re^{n_2}$ are independent, then they, together with S''s sample point $A\mathbf{p}$, *might* represent an $(n_2 - 1)$-dimensional facet bordering the projected halfspace intersection.

To test whether S' is indeed on the projected volume's boundary, we proceed to step (3) of our task. Figure 2 depicts the projection of an intersection of halfspaces from $\Re^3$ into $\Re^2$. Of interest are the three halfspaces $\Gamma_1(\mathbf{n}_1, d_1)$, $\Gamma_2(\mathbf{n}_2, d_2)$, and $\Gamma_3(\mathbf{n}_3, d_3)$. 1-dimensional Facet S_1, formed by intersecting the planes bounding the halfspaces $\Gamma_1(\mathbf{n}_1, d_1)$ and $\Gamma_2(\mathbf{n}_2, d_2)$, has affine space basis $\{\mathbf{u}_1\} \perp \mathbf{n}_1, \mathbf{n}_2$. S_1 projects to boundary facet S_1', with affine space basis $\{A\mathbf{u}_1\}$. S_1' lies on the boundary of the projected

volume. To characterize S', unit normal $\mathbf{n}'_1$ to S'_1's surface is easily derived as $A\mathbf{u}_1$'s perpendicular in $\Re^{n_2}$, and $d'_1 = A\mathbf{p}_1 \cdot \mathbf{n}'_1$ gives S''s distance to the origin of $\Re^{n_2}$. Facet S_2 is formed by intersecting the planes bounding halfspaces $\Gamma_2(\mathbf{n}_2, d_2)$ and $\Gamma_3(\mathbf{n}_3, d_3)$. S_2 projects to S'_2, whose affine space passes through the interior of the projected volume. S'_2 is similarly characterized by normal $\mathbf{n}'_2$ and scalar d'_2.

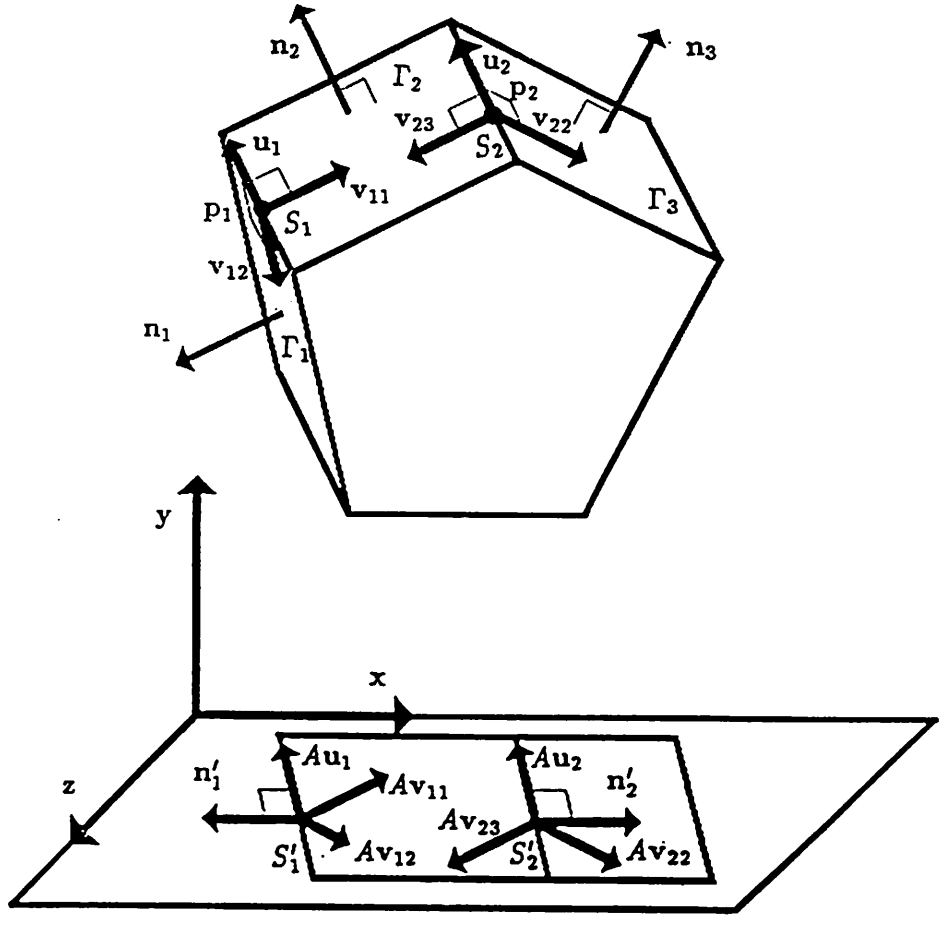

Figure 2. Projecting an intersection of $\Re^3$-halfspaces onto the xy-plane

To appreciate intuitively why S_1, but not S_2, projects to form a boundary facet, define $\mathbf{v}_{11} \perp \mathbf{u}_1, \mathbf{n}_2$ and $\mathbf{v}_{12} \perp \mathbf{u}_1, \mathbf{n}_1$ (see figure 2). Any point $\mathbf{q}$ lying in the intersection of the two halfspaces $\Gamma_1(\mathbf{n}_1, d_1)$ and $\Gamma_2(\mathbf{n}_2, d_2)$ may be expressed as the vector sum $\mathbf{q} = \mathbf{p}_1 + a_1\mathbf{u}_1 + b_{11}\mathbf{v}_{11} + b_{12}\mathbf{v}_{12}$, where $\mathbf{p}_1$ is a point on S_1, $a_1 \in \Re$, and $b_{11}, b_{12} \in \Re^+$. As is apparent in figure 2, every such point $\mathbf{q}$ projects to the same side of S', i.e., $\mathbf{n}_1' \cdot A\mathbf{q} \leq \mathbf{n}_1' \cdot A\mathbf{p}_1$.

On the other hand, any point $\mathbf{q}$ lying in $\Gamma_2(\mathbf{n}_2, d_2) \bigcap \Gamma_3(\mathbf{n}_3, d_3)$ may be expressed as $\mathbf{q} = \mathbf{p}_2 + a_2\mathbf{u}_2 + b_{22}\mathbf{v}_{22} + b_{23}\mathbf{v}_{23}$, where $\mathbf{p}_2$ is a point on S_2, $a_1 \in \Re$, $b_{11}, b_{12} \in \Re^+$, and $\mathbf{v}_{22} \perp \mathbf{u}_2, \mathbf{n}_3$, $\mathbf{v}_{23} \perp \mathbf{u}_2, \mathbf{n}_2$. Two such points, $\mathbf{p}_2 + \mathbf{v}_{22}$ and $\mathbf{p}_2 + \mathbf{v}_{23}$, project to opposite sides of S_2'. That is, $\mathbf{n}_2' \cdot A(\mathbf{p}_2 + \mathbf{v}_{22}) < \mathbf{n}_2' \cdot A\mathbf{p}_2$. but $\mathbf{n}_2' \cdot A(\mathbf{p}_2 + \mathbf{v}_{23}) > \mathbf{n}_2' \cdot A\mathbf{p}_2$. More directly, S_1' lies on the boundary of the projected volume because $\mathbf{n}_1' \cdot A\mathbf{v}_{11}$ and $\mathbf{n}_1' \cdot A\mathbf{v}_{12}$ are of the same sign. S_2' does not lie on the boundary because $\mathbf{n}_2' \cdot A\mathbf{v}_{22}$ and $\mathbf{n}_2' \cdot A\mathbf{v}_{23}$ are opposite in sign.

The above observations are generalized and presented formally in theorems 1 and 2. Theorem 1 formally justifies the above characterization of any point $\mathbf{q}$ in the intersection of k $\Re^{n_1}$-halfspaces as a weighted sum of a point $\mathbf{p} \in S$, S basis vectors $\mathbf{u}_1, \ldots, \mathbf{u}_{n_1-k}$, and tangent vectors $\mathbf{v}_1, \ldots, \mathbf{v}_k$. Theorem 2 formalizes the argument that an $(n_2 - 1)$-dimensional facet S's projection S' into $\Re^{n_2}$ lies on the projected volume's border iff all of the vectors $\mathbf{v}_i$ project to the same side of S'.

Theorem 1. Let $\Gamma_1(\mathbf{n}_1, d_1), \ldots, \Gamma_k(\mathbf{n}_k, d_k)$ denote $k > 1$ hyperplanar halfspaces in $\Re^n$, such that $\mathbf{x} \in \Re^n$ is in halfspace $\Gamma_i(\mathbf{n}_i, d_i)$ iff $\mathbf{n}_i \cdot \mathbf{x} \leq d_i$, with $\mathbf{n} \in \Re^n$ and $d_i \in \Re$. Let the k hyperplanes bounding halfspaces $\Gamma_1, \ldots, \Gamma_k$ intersect at $S = \{\mathbf{x} \in \Re^n \mid \mathbf{n}_1 \cdot \mathbf{x} = d_1, \ldots, \mathbf{n}_k \cdot \mathbf{x} = d_k\}$. Suppose $\mathbf{n}_1, \ldots, \mathbf{n}_k$ are independent in $\Re^n$, so S can be expressed as the $(n - k)$-dimensional affine space $S = \{\mathbf{x} \in \Re^n \mid \mathbf{x} = \mathbf{p} + \sum_{j=1}^{n-k} a_j\mathbf{u}_j,\ a_j \in \Re\}$, where $\mathbf{p}$ is a

point on S and $\mathbf{u}_1, \ldots, \mathbf{u}_{n-k} \in \Re^n$ form a basis for S. Define $\mathbf{v}_1, \ldots, \mathbf{v}_k \in \Re^n$ such that for $j = 1 \ldots k$, $\mathbf{v}_j \perp \mathbf{n}_1, \ldots, \mathbf{n}_{j-1}, \mathbf{n}_{j+1}, \ldots, \mathbf{n}_k, \mathbf{u}_1, \ldots, \mathbf{u}_{n-k}$ and $\mathbf{v}_j \cdot \mathbf{n}_j < 0$. Then for any $\mathbf{q} \in \Re_n$, $\mathbf{q} \cdot \mathbf{n}_i \leq d_i, i = 1 \ldots k$ iff $\mathbf{q}$ can be expressed as $\mathbf{q} = \mathbf{p} + \sum_{j=1}^{n-k} a_j \mathbf{u}_j + \sum_{j=1}^{k} b_j \mathbf{v}_j$, with $a_j \in \Re, b_j \in \Re^+$.

Proof:

$\Rightarrow$: The vectors $\mathbf{u}_1, \ldots, \mathbf{u}_{n-k}, \mathbf{v}_1, \ldots, \mathbf{v}_k$ are clearly independent, so they form a basis for $\Re^n$. Hence, for any $\mathbf{q} \in \Re^n$, $\mathbf{q} = \mathbf{p} + \sum_{j=1}^{n-k} a_j \mathbf{u}_j + \sum_{j=1}^{k} b_j \mathbf{v}_j$, with $a_j \in \Re, b_j \in \Re$. Now it suffices to show that $b_j \geq 0, j = 1 \ldots k$. We are given that $\mathbf{q} \cdot \mathbf{n}_i \leq d_i, i = 1 \ldots k$, so $(\mathbf{p} + \sum_{j=1}^{n-k} a_j \mathbf{u}_j + \sum_{j=1}^{k} b_j \mathbf{v}_j) \cdot \mathbf{n}_i \leq d_i$, $i = 1 \ldots k$. And $\mathbf{p} \cdot \mathbf{n}_i = d_i$, so $(\sum_{j=1}^{n-k} a_j \mathbf{u}_j) \cdot \mathbf{n}_i + (\sum_{j=1}^{k} b_j \mathbf{v}_j) \cdot \mathbf{n}_i \leq 0$, $i = 1 \ldots k$. But $\mathbf{u}_j \cdot \mathbf{n}_i = 0$ for $i \in 1 \ldots k$ $j \in 1 \ldots n-k$ and $\mathbf{v}_j \cdot \mathbf{n}_i = 0$ for $i \neq j$, so $b_i \mathbf{v}_i \cdot \mathbf{n}_i \leq 0, i = 1 \ldots k$. Moreover, we are also given that $\mathbf{v}_i \cdot \mathbf{n}_i < 0$, so $b_i \geq 0, i = 1 \ldots k$.

$\Leftarrow$: Assume $\mathbf{q} = \mathbf{p} + \sum_{j=1}^{n-k} a_j \mathbf{u}_j + \sum_{j=1}^{k} b_j \mathbf{v}_j$, with $a_j \in \Re, b_j \in \Re^+$. Since $\mathbf{u}_j \cdot \mathbf{n}_i = 0$ for $i, j \in 1, \ldots, n$ and $\mathbf{v}_j \cdot \mathbf{n}_i = 0$ for $i \neq j$, if follows that $\mathbf{q} \cdot \mathbf{n}_i = \mathbf{p} \cdot \mathbf{n}_i + b_i \mathbf{v}_i \cdot \mathbf{n}_i$, with $b_i \geq 0$, $i = 1, \ldots k$. In fact, $\mathbf{q} \cdot \mathbf{n}_i = d_i + b_i \mathbf{v}_i \cdot \mathbf{n}_i$, with $b_i \geq 0$, $i = 1, \ldots k$. And $\mathbf{v}_i \cdot \mathbf{n}_i < 0$, so $b_i \mathbf{v}_i \cdot \mathbf{n}_i \leq 0$. We may therefore conclude that $\mathbf{q} \cdot \mathbf{n}_i \leq d_i, i = 1, \ldots k$. □

Theorem 1'. The open set version of theorem 1, in which the relation $\leq$ is replaced by $<$ throughout, and $b_j > 0$, is stated similarly to theorem 1, with an analogous proof.

Theorem 2. Let $k > 1$ halfspaces $\Gamma_1(\mathbf{n}_1, d_1), \ldots, \Gamma_k(\mathbf{n}_k, d_k)$, affine space S, its basis $\mathbf{u}_1, \ldots, \mathbf{u}_{n-k}$, point $\mathbf{p} \in S$, and vectors $\mathbf{v}_1, \ldots, \mathbf{v}_k$ be as defined in theorem 1. Now let A be an $(n-k+1) \times n$ matrix. Suppose the vectors $A\mathbf{u}_1, \ldots A\mathbf{u}_{n-k}$ are independent and thus form a basis for $\Re^{n-k}$. Define $\mathbf{n}' \in \Re^{n-k+1}$ such that $\mathbf{n}' \perp A\mathbf{u}_1, \ldots A\mathbf{u}_{n-k}$, and let $A\mathbf{p} \cdot \mathbf{n}' = d'$. Then

$A\mathbf{v}_i \cdot \mathbf{n}' \leq 0$ for $i = 1 \ldots k$ (or $\geq$ respectively) iff for all $\mathbf{q} \in \bigcap_{i=1}^{k} \Gamma_i(\mathbf{n}_i, d_i)$, $A\mathbf{q} \cdot \mathbf{n}' \leq d'$ (or $\geq$ respectively).

Proof:

$\Rightarrow$: Assume $A\mathbf{v}_i \cdot \mathbf{n}' \leq 0$ and $\mathbf{q} \cdot \mathbf{n}_i \leq d_i$, $i = 1 \ldots k$. By theorem 1, $\mathbf{q}$ may be expressed as $\mathbf{q} = \mathbf{p} + \sum_{j=1}^{n-k} a_j \mathbf{u}_j + \sum_{j=1}^{k} b_j \mathbf{v}_j$, with $a_j \in \Re, b_j \in \Re^+$. then A maps $\mathbf{q}$ to $A\mathbf{p} + \sum_{j=1}^{n-k} a_j A\mathbf{u}_j + \sum_{j=1}^{k} b_j A\mathbf{v}_j$, with $a_j \in \Re, b_j \in \Re^+$. Therefore, $A\mathbf{q} \cdot \mathbf{n}' = A\mathbf{p} \cdot \mathbf{n}' + \sum_{j=1}^{n-k} a_j A\mathbf{u}_j \cdot \mathbf{n}' + \sum_{j=1}^{k} b_j A\mathbf{v}_j \cdot \mathbf{n}'$, with $a_j \in \Re, b_j \in \Re^+$. But $A\mathbf{p} \cdot \mathbf{n}' = d'$ and $A\mathbf{u}_j \cdot \mathbf{n}' = 0, j = 1 \ldots n-k$, so $A\mathbf{q} \cdot \mathbf{n}' = d' + \sum_{j=1}^{k} b_j A\mathbf{v}_j \cdot \mathbf{n}'$, with $b_j \in \Re^+$. Given that $A\mathbf{v}_i \cdot \mathbf{n}' \leq 0$ and $b_j \geq 0$, we conclude that $A\mathbf{q} \cdot \mathbf{n}' \leq d'$. The respective case where we assume $A\mathbf{v}_i \cdot \mathbf{n}' \geq 0$ similarly leads to $A\mathbf{q} \cdot \mathbf{n}' \geq d'$.

$\Leftarrow$: Let $\mathbf{q} = \mathbf{p} + \mathbf{v}_{i_0}$ for any $i_0 \in 1 \ldots k$. Noting that for all $i \in 1 \ldots k$, $\mathbf{p} \cdot \mathbf{n}_i = d_i$, $\mathbf{v}_{i_0} \cdot \mathbf{n}_i = 0$ when $i_0 \neq i$, and $\mathbf{v}_{i_0} \cdot \mathbf{n}_i < 0$ when $i_0 = i$, it follows that $\mathbf{q} \cdot \mathbf{n}_i \leq d_i$ for $i \in 1 \ldots k$. We may then conclude that $A\mathbf{q} \cdot \mathbf{n}' \leq d'$, i.e., that $A\mathbf{p} \cdot \mathbf{n}' + A\mathbf{v}_{i_0} \cdot \mathbf{n}' \leq d'$. But $A\mathbf{p} = d'$, so $A\mathbf{v}_{i_0} \cdot \mathbf{n}' \leq 0$. □

Theorem 2*. The open set version of theorem 2, in which the relation $\leq$ is replaced by $<$ throughout, and $b_j > 0$, is stated similarly to theorem 2, with an analogous proof that utilizes theorem 1* where theorem theorem 2 employs theorem 1.

Theorem 2 suggests an algorithm, presented below, for projecting an intersection of halfspaces from $\Re^{n_1}$ into $\Re^{n_2}$. The algorithm examines each $(n_2 - 1)$-dimensional facet of the intersection volume in $\Re^{n_1}$, to determine, according to theorem 2, if its projection lies on the boundary of the projected volume in $\Re^{n_2}$. The algorithm is presented with an emphasis on clarity, at the expense of efficiency.

HALFSPACE INTERSECTION PROJECTION PROCEDURE

Input: m_1 $\Re^{n_1}$-halfspaces $\Gamma_1(\mathbf{n}_1, d_1), \ldots, \Gamma_{m_1}(\mathbf{n}_{m_1}, d_{m_1})$ and $n_2 \times n_1$ projecton matrix A

Output: List $HSPACES$ containing some $m_2 \geq 0$ $\Re^{n_2}$-halfspaces which bound the $\Re^{n_1}$-halfspace intersection's projection by matrix A

```
Begin
  Initialize HSPACES as an empty list
  Let k = n1 − n2 + 1
  For each k-tuple (Γ1(n1, d1), ..., Γk(nk, dk))
    If n1, ..., nk are independent
      then
        GS_{n1}(n1, ..., nk) → u1, ..., u_{n2−1}
        If Au1, ..., Au_{n2−1} are independent
          then
            Solve the n1 × n1 system of equations for p:
              ni · p = di,   i = 1...k
              ui · p = 0,    i = 1...n2 − 1
            PERP_{n2}(Au1, ..., Au_{n2−1}) → n'
            For i from 1 to k do
              PERP_{n1}(n1, ..., n_{i−1}, n_{i+1}, ..., nk, u1, ..., u_{n2−1}) → vi
              If vi · ni > 0  then  −vi → vi  Endif
            Endfor
            If n' · Avi ≤ 0 for i = 1...k
              then
                insert Γ(n', Ap) into HSPACES
            Elseif n' · Avi ≥ 0 for i = 1...k
              then
                insert Γ(−n', −Ap) into HSPACES
            Else /*not a bounding halfspace*/
            Endif
        Endif
    Endif
  Endfor
  Return list HSPACES
End
```

The above algorithm makes use of subroutine $GS_n(\mathbf{w}_1, \ldots, \mathbf{w}_m)$, which uses the Gram-Schmidt technique (see [4]) to find $n-m$ orthogonal vectors in $\Re^n$ that are orthogonal to m vectors $\mathbf{w}_1, \ldots, \mathbf{w}_m$ in $\Re^n$ $(m < n)$. Procedure $PERP_n(\mathbf{w}_1, \ldots, \mathbf{w}_{n-1})$ is also employed, to compute one of the two vectors $\mathbf{w}_n$ in $\Re^n$ orthogonal to all of $\mathbf{w}_1, \ldots, \mathbf{w}_{n-1}$. $PERP_n$ solves the $n \times n$ system of equations $\mathbf{w}_i \cdot \mathbf{w}_n = 0, i = 1 \ldots n-1, \mathbf{a} \cdot \mathbf{w}_n = 0$, where $\mathbf{a}$ is the standard axis in $\Re^n$ whose angle with the closest of the $\mathbf{w}_i$ is maximal.

The projection algorithm iteratively examines each $(n_2 - 1)$-dimensional facet S of the volume in $\Re^{n_1}$ defined by the intersection of k halfspaces. Each k-tuple of halfspaces $\Gamma_1(\mathbf{n}_1, d), \ldots, \Gamma_k(\mathbf{n}_k, d_k)$ forms an $(n_2 - 1)$-dimensional affine space $\mathcal{A}$, which may or may not correspond to an $(n_2 - 1)$-dimensional boundary facet S of the intersection volume. $\mathcal{A}$ has basis $\mathbf{u}_1, \ldots, \mathbf{u}_{n_2-1} \perp \mathbf{n}_1, \ldots, \mathbf{n}_k$, computed via gram-schmidt procedure GS_{n_1}, and representative point $\mathbf{p}$, computed by solving an $n_1 \times n_1$ system of linear equations. If the projected basis vectors $A\mathbf{u}_1, \ldots, A\mathbf{u}_{n_2-1}$ are independent in $\Re^{n_2}$, then they form the basis for an $(n_2 - 1)$-dimensional affine space $\mathcal{A}'$, with representative point $A\mathbf{p}$. A vector $\mathbf{n}'$ orthogonal to $A\mathbf{u}_1, \ldots, A\mathbf{u}_{n_2-1}$ is computed by $PERP_{n_2}$.

Assuming the affine space $\mathcal{A}$ contains a bording facet S of the original volume in $\Re_{n_1}$, theorem 2 provides a test to see whether the projection $\mathcal{A}'$ of $\mathcal{A}$ in turn forms a bordering facet S' of the projected volume in $\Re^{n_2}$. $PERP_{n_1}$ provides the k vectors $\mathbf{v}_i$ defined in theorem 2, and the test amounts to deciding whether or not all k projections $A\mathbf{v}_i$ lie on the same side of $\mathcal{A}'$. If so, then the halfspace $\{\mathbf{x} \in \Re^{n_2} \mid \mathbf{n}' \cdot \mathbf{x} \leq A\mathbf{p}\}$ or $\{\mathbf{x} \in \Re^{n_2} \mid -\mathbf{n}' \cdot \mathbf{x} \leq -A\mathbf{p}\}$ (depending on the side of $\mathcal{A}'$ to which the $\mathbf{v}_i$ project) is submitted tentatively as a bounding halfspace in the projected volume's description $HSPACES$. If $\mathcal{A}$ did not contain a boundary facet S of the original volume in $\Re^{n_1}$, then the latter halfspace is redundant. Redundant halfspaces may be detected via linear programming if desired, and discarded from $HSPACES$.

Computational Complexity

The computational cost of the halfspace intersection projection algorithm can be analyzed in terms of the number of primitive arithmetic operations $(+,-,\times,\div)$ required. To project the intersection of m_1 halfspaces from $\Re^{n_1}$ into $\Re^{n_2}$, there are $\frac{m_1!}{k!(m_1-k)!}$ k-tuples of halfspaces to consider, where $k = n_1 - n_2 + 1$. The complexity of processing each k-tuple is analyzed as follows.

Operation $GS_{n_1}(\mathbf{n}_1, \ldots \mathbf{n}_k)$ applies the Gram-Schmidt orthogonalization process to n_1 vectors $\mathbf{n}_1, \ldots \mathbf{n}_k, \mathbf{a}_1, \ldots \mathbf{a}_{n_2-1}$, where $\mathbf{a}_1, \ldots \mathbf{a}_{n_2-1}$ are the n_2-1 standard unit axes in $\Re^{n_1}$ that form the greatest angle (for numerical reasons) to the vector space spanned by $\mathbf{n}_1, \ldots \mathbf{n}_k$. A Gram-Schmidt orthogonalization of n_1 vectors in $\Re^{n_1}$ would generally require $\mathcal{O}(n_1^2)$ dot products, resulting in $\mathcal{O}(n_1^3)$ primitive operations. The dot products involving the unit axes $\mathbf{a}_i$, however, can be performed as simple vector element access operations, so GS_{n_1} requires only $\mathcal{O}(k^3)$ time. The check for the indepedence of $\mathbf{n}_1, \ldots \mathbf{n}_k$ is also done during the GS_{n_1} routine, which detects dependence when $\mathbf{u}_i = 0$ for some i.

Each system of linear equations in the algorithm can be solved in $\mathcal{O}(n_1^2)$ time. There are $k+2$ such systems per k-tuple, so the time spent solving simultaneous equations is $\mathcal{O}(kn_1^2)$. Finally, there are n_1 vector projections $A\mathbf{w}_i$ by $n_2 \times n_1$ matrix A, each requiring $\mathcal{O}(n_1 n_2)$ primitive operations, so $\mathcal{O}(n_1^2 n_2)$ time is required for projecting vectors.

Each k-tuple is therfore processed in $\mathcal{O}(k^3 + kn_1^2 + n_1^2 n_2)$ time, and the entire algorithm takes $\mathcal{O}\left(\frac{m_1!}{k!(m_1-k)!}(k^3 + kn_1^2 + n_1^2 n_2)\right)$ time.

4 What do the resulting constraints guarantee?

In this section, we explore what the constraints defining a linear constraint volume's projection into a lower-dimensional space can and cannot guarantee regarding the satisfaction of the higher-dimensional constraints.

As illustrated in figure 2, the hyperplanes associated with halfspaces $\Gamma(\mathbf{n}_1, d_1)$ and $\Gamma(\mathbf{n}_2, d_2)$ intersect at face S_1, whose projection S_1' forms a bordering facet of the projected volume. Any point $\mathbf{q}$ residing in the intersection of $\Gamma(\mathbf{n}_1, d_1)$ and $\Gamma(\mathbf{n}_2, d_2)$ must project to S_1' or the interior (right) side of S_1'. But as we readily observe in figure 2, the projection of a point $\mathbf{q}$ to S_1' or the interior side of S_1' does not guarantee $\mathbf{q}$'s residence in both of $\Gamma(\mathbf{n}_1, d_1)$ and $\Gamma(\mathbf{n}_2, d_2)$. Owing to the nonzero nullity of the projection matrix, $\mathbf{q}$ is underdetermined by its projected image.

Theorems 3 and 4 formalize these observations for general projections from $\Re^{n_1}$ to $\Re^{n_2}$, where $n_1 > n_2$. Suppose the hyperplanes associated with k halfspaces in $\Re^{n_1}$ intersect to form an $(n_2 - 1)$ -dimensional facet S whose projection S' forms a bordering facet of the projected constraint volume in $\Re^{n_2}$, as required by theorem 2. Theorem 3 tells us that if $\mathbf{q} \in \Re^{n_1}$ lies outside of all k halfspaces, then $\mathbf{q}$ must project to the exterior side of S'. The corollary to theorem 3 asserts that $\mathbf{q}$ must satisfy at least one of the k halfspace constraints in $\Re^{n_1}$ if it projects to S' or the interior side of S'. Finally, theorem 4 states that $\mathbf{q}$ need not lie in more than one of the k halfspaces $\Gamma(\mathbf{n}_i, d_i)$ for its projection to fall on S' or the interior side of S'.

Theorem 3. Let $k > 1$ halfspaces $\Gamma_1(\mathbf{n}_1, d_1), \ldots, \Gamma_k(\mathbf{n}_k, d_k)$, affine space S, its basis $\mathbf{u}_1, \ldots, \mathbf{u}_{n-k}$, point $\mathbf{p} \in S$, vectors $\mathbf{v}_1, \ldots, \mathbf{v}_k$, $(n-k+1) \times n$ matrix A, $\mathbf{n}' \in \Re^{n-k+1}$, and $d' \in \Re$ be defined as in theorems 1 and 2. Suppose $A\mathbf{v}_i \cdot \mathbf{n}' \leq 0$ for $i = 1 \ldots k$, and let $\mathbf{q} \in \Re^{n_1}$, with $\mathbf{q} \cdot \mathbf{n}_i > d_i$ for $i = 1 \ldots n$. Then $A\mathbf{q} \cdot \mathbf{n}' > d'$.

Proof:

Let $\bar{\Gamma}_1(-\mathbf{n}_1, -d_1), \ldots, \bar{\Gamma}_k(-\mathbf{n}_k, -d_k)$ denote k hyperplanar halfspaces in $\Re^n$ such that $\mathbf{x} \in \Re^n$ is in halfspace $\bar{\Gamma}_i(-\mathbf{n}_i, -d_i)$ iff $-\mathbf{n}_i \cdot \mathbf{x} < -d$. For $j = 1 \ldots k$, $-\mathbf{v}_j \perp -\mathbf{n}_1, \ldots, -\mathbf{n}_{j-1}, -\mathbf{n}_{j+1}, \ldots, -\mathbf{n}_k, \mathbf{u}_1, \ldots, \mathbf{u}_{n-k}$, and $-\mathbf{v}_j \cdot -\mathbf{n}_j < 0$. Note that $A\mathbf{p} \cdot (-\mathbf{n}') = -d'$ and $A(-\mathbf{v}_i) \cdot (-\mathbf{n}') < 0$ for $i = 1 \ldots k$. Hence, by theorem 2*, if $\mathbf{q} \in \bigcap_{i=1}^{k} \bar{\Gamma}_i(-\mathbf{n}_i, -d_i)$, then $A\mathbf{q} \cdot -\mathbf{n}' < -d'$. But we are given $\mathbf{q} \cdot \mathbf{n}_i > d_i$, i.e., $\mathbf{q} \cdot (-\mathbf{n}_i) < -d_i$, $i = 1 \ldots k$, so $\mathbf{q} \in \bigcap_{i=1}^{k} \bar{\Gamma}_i(-\mathbf{n}_i, -d_i)$. Hence, $A\mathbf{q} \cdot -\mathbf{n}' < -d'$, i.e., $A\mathbf{q} \cdot \mathbf{n}' > d'$. □

Corollary. If $A\mathbf{q} \cdot \mathbf{n}' \leq d'$, then $\mathbf{q} \cdot \mathbf{n}_i \leq d_i$ for some $i \in 1 \ldots n$.

Proof:

If $\mathbf{q} \cdot \mathbf{n}_i > d_i$ for $i = 1 \ldots n$, then by theorem 3, $A\mathbf{q} \cdot \mathbf{n}' > d'$. □

Theorem 4. Let $k > 1$ halfspaces $\Gamma_1(\mathbf{n}_1, d_1), \ldots, \Gamma_k(\mathbf{n}_k, d_k)$, affine space S, its basis $\mathbf{u}_1, \ldots, \mathbf{u}_{n-k}$, point $\mathbf{p} \in S$, vectors $\mathbf{v}_1, \ldots, \mathbf{v}_k$, $(n-k+1) \times n$ matrix A, $\mathbf{n}' \in \Re^{n-k+1}$, and $d' \in \Re$ be defined as in theorems 1 and 2. Suppose $A\mathbf{v}_i \cdot \mathbf{n}' \leq 0$ for $i = 1 \ldots k$. Let $r \leq n - k + 1$ be the rank of A and $\mathcal{N}(A)$ be the nullspace of A. Let $\Gamma_{i_1}(\mathbf{n}_{i_1}, d_{i_1}), \ldots, \Gamma_{i_h}(\mathbf{n}_{i_h}, d_{i_h})$ be $h < k$ of the k halfspaces $\Gamma_i(\mathbf{n}_i, d_i)$ such that for $j = 1 \ldots h$, $\mathbf{n}_{i_j}$ is nonorthogonal to $\mathcal{N}(A)$. Then there exists a point $\mathbf{q} \in \Re^n$ such that $A\mathbf{q} \cdot \mathbf{n}' \leq d'$ and $\mathbf{q} \cdot \mathbf{n}_{i_j} > d_{i_j}$ for $j = 1 \ldots h$.

Proof:

A has nullity $n - r$. Let $\mathcal{N}(A)$ have basis $\mathbf{w}_1, \ldots, \mathbf{w}_{n-r}$. Form the $h \times (n-r)$ system equations

$$\begin{aligned} (a_1\mathbf{w}_1 + \cdots + a_{n-r}\mathbf{w}_{n-r}) \cdot \mathbf{n}_{i_1} &= c_1 \\ &\vdots \\ (a_1\mathbf{w}_1 + \cdots + a_{n-r}\mathbf{w}_{n-r}) \cdot \mathbf{n}_{i_h} &= c_h \end{aligned}$$

in variables $a_1, \ldots, a_{n-r}$, with $c_i > 0, i \in 1, \ldots, h$. Since $r \leq n - k + 1$, this

system has $n - r \geq k - 1$ columns. It also has $h \leq k - 1$ rows, so the system has a solution $\bar{a}_1, \ldots \bar{a}_{n-r}$. Let $\mathbf{q} = \mathbf{p} + \bar{a}_1 \mathbf{w}_1 + \cdots + \bar{a}_{n-r} \mathbf{w}_{n-r}$. By p's definition, $\mathbf{p} \cdot \mathbf{n}_i = 0$ for $i = 1 \ldots k$, so $\mathbf{q} \cdot \mathbf{n}_{i_j} = c_{i_j} > 0$ for $j = 1, \ldots, h$. Finally, $A\mathbf{q} = A\mathbf{p}$ and $A\mathbf{p} \cdot \mathbf{n}' = d'$, so $A\mathbf{q} \cdot \mathbf{n}' \leq d'$. □

Corollary. If none of the k normals $\mathbf{n}_i$ is orthogonal to $\mathcal{N}(A)$, then for any $(k-1)$-tuple $\mathbf{n}_{i_1}, \ldots, \mathbf{n}_{i_{k-1}}$ of the k normals, there exists a point $\mathbf{q} \in \Re^n$ such that $A\mathbf{q} \cdot \mathbf{n}' \leq d'$ and $\mathbf{q} \cdot \mathbf{n}_{i_j} > d_{i_j}$, $j = 1 \ldots k-1$.

Proof:
This follows immediately from theorem 3, with $h = k - 1$. □

5 Application to computing applied force constraints in 3-D

In this section we extend the technique for deriving applied force constraints presented in section 2 to handle single and multiple insertion tasks in the 3-dimensional polyhedral world. We employ the projection algorithm described in section 3 to project intersections of contact force halfspaces into 6-dimensional applied force space. As proven in section 4, the resulting wrench constraints provide necessary, though not sufficient, conditions for satisfying all contact force constraints.

We first enumerate the possible types of contact that can occur during the insertion, along with an associated set of contact force constraints.

The three primitive types of contact that can occur between the boundary features of a polyhedral insertor (peg) and a polyhdral container (hole) are (1) a *vertex-face* contact, in which an insertor vertex contacts a planar face of the container, (2) a *face-vertex* contact, in which a planar face of the insertor contacts a vertex of the container, and (3) an *edge-edge* contact, where an insertor edge contacts a container edge. From a purely kinematic

point of view, it can be shown that all other contacts occuring between two polyhedral objects are expressible as combinations of these primitive contacts. In this report, we will only consider point-contact combinations, i.e., those not involving areal or line contacts. This will enable us to make use of very straightforward statics when deriving the projection matrix.

Figure 3 shows a vertex-face contact occuring between an insertor vertex at point P and a planar face F with outward surface normal $\mathbf{n}$. Face F exerts a reaction force $\mathbf{f}$ against the vertex. The friction cone surrounding $\mathbf{n}$ contains the set of reaction forces that face F can exert. Reaction forces in the cone's interior are associated with static friction (jamming), and reaction forces on the cone's surface are associated with sliding friction. Figure 3 shows the desired direction $\mathbf{m}$ for the sliding motion of the vertex. We wish to construct linear inequalities to constrain $\mathbf{f}$ and thereby attempt to avoid various failure modes. Our requirements are that the vertex must (1) not break contact with face F, (2) not exert a force whose magnitude exceeds f_{max}, (3) slide in the positive $\mathbf{m}$-direction without jamming on the surface of F.

Constraint surfaces imposing these restrictions on $\mathbf{f}$ are shown in figure 3. The breaking of contact is avoided by restricting $\mathbf{f}$ to the halfspace defined by the inequality $\mathbf{n} \cdot \mathbf{f} \geq f_{min}$ where bias force $f_{min} > 0$ ensures a nonzero reaction force. This halfspace is represented by constraint plane Γ_1 in figure 3. The constraint on the reaction force's magnitude is similarly represented by the inequality $\mathbf{n} \cdot \mathbf{f} \leq f_{max}$, with associated constraint surface Γ_2. A jamming avoidance constraint plane Γ_3 tangent to the friction cone's surface and opposite to $\mathbf{m}$ prevents jamming and guarantees that the vertex will slide in the positive $\mathbf{m}$-direction. The inequality $(-\mathbf{m}\cos\theta - \mathbf{n}\sin\theta) \cdot \mathbf{f} \geq 0$ describes this final constraint, where $\sin\theta$ is the coefficient of friction.

The contact force constraint inequalities for face-vertex contacts are the same as for vertex-face contacts, but with the face's surface normal negated.

Inequalties for edge-edge contacts are the same as for vertex-plane contacts, except that $\mathbf{v}_1 \times \mathbf{v}_2$ or $\mathbf{v}_2 \times \mathbf{v}_1$ serves as the surface normal, where $\mathbf{v}_1$ and $\mathbf{v}_2$ are the insertor and container edge direction vectors, respectively.

The n point-contact forces $\mathbf{f}_1, \ldots, \mathbf{f}_n$ relate to the 6-dimensional, applied object force $\mathbf{F}$ through a $6 \times 3n$ quasi-statics matrix:

$$\mathbf{F} = \begin{pmatrix} F_x \\ F_y \\ F_z \\ M_x \\ M_y \\ M_z \end{pmatrix} = \begin{pmatrix} -\mathbf{I} & \cdots & -\mathbf{I} \\ -\mathbf{r}_1\times & \cdots & -\mathbf{r}_n\times \end{pmatrix} \begin{pmatrix} \mathbf{f}_1 \\ \vdots \\ \mathbf{f}_n \end{pmatrix} \tag{4}$$

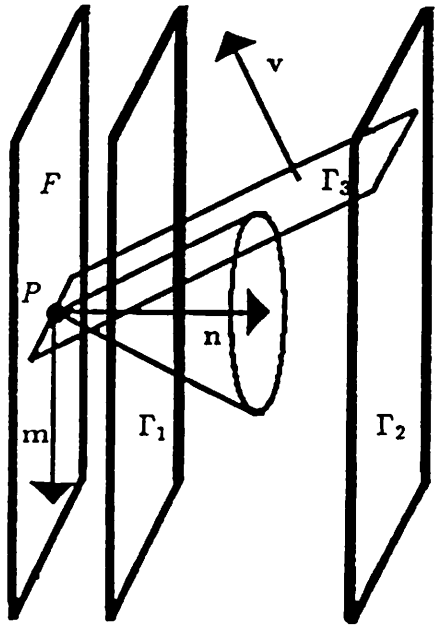

Figure 3. Reaction force constraints for a vertex-face contact

where I denotes a 3×3 identity matrix, and $\mathbf{r}_i\times$ denotes a 3×3 cross product matrix constructed for the position $\mathbf{r}_i$ of the contact point, expressed in insertor's coordinate frame. To conform with equation (4)'s $3n$-dimensional respresentation of contact force combinations, constraint inequalities of the form $\mathbf{n}_i \cdot \mathbf{f}_i \leq d_i$ over the ith contact force can be expressed in $\mathbf{f}_1 \times \cdots \times \mathbf{f}_n$-space as the inequality

$$\begin{pmatrix} 0_1^T & \cdots & 0_{i-1}^T & \mathbf{n}_i^T & 0_{i+1}^T & \cdots & 0_n^T \end{pmatrix} \begin{pmatrix} \mathbf{f}_1 \\ \vdots \\ \mathbf{f}_n \end{pmatrix} \leq d_i$$

where 0 denotes the zero vector in 3-space.

Figure 4 shows a contact state that might occur during the insertion of a square peg into a square hole. The configuration shown represents a differential perturbation from an ideal configuration and geometry in which the peg's square base coincides exactly with the hole's square rim, the dimensions of the two squares being equal. A small perturbation of the hole's lateral dimensions produces a differential clearance that permits the peg to tilt differentially about its three axes. In the perturbed configuration, the peg contacts the hole's interior at three points. Peg edge E_1 contacts hole edge E_1' at point P_1, Peg edge E_2 contacts hole edge E_2' at point P_2, and the peg vertex at P_3 contacts hole face F.

We now construct contact force constraints for this 3-point contact state, using contact points and surface features associated with the ideal configuration and geometry. The ideal directions of peg edge E_1 and hole edge E_1' are the y axis and x axis, respectively, so the normal force for the edge-edge contact at P_1 is nominally directed along $\mathbf{n}_1 = \mathbf{y} \times \mathbf{x} = -\mathbf{z}$. The normal force for the edge-edge contact at P_2 is nominally directed along $\mathbf{n}_2 = \mathbf{z} \times \mathbf{y} = -\mathbf{x}$. The normal force for the vertex-face contact at P_3 is nominally directed along F's normal $\mathbf{n} = \mathbf{x}$.

Using the formula $\mathbf{n} \cdot \mathbf{f} \geq f_{min}$, the constraints for not breaking contact at P_1,P_2, and P_3 are (1) $-f_{1z} \geq f_{min}$, (2) $-f_{2x} \geq f_{min}$, and (3) $f_{3x} \geq f_{min}$. The formula $\mathbf{n} \cdot \mathbf{f} \leq f_{max}$ for avoiding excess stress at the contacts similarly yields (4) $-f_{1z} \leq f_{max}$, (5) $-f_{2x} \leq f_{max}$, and (6) $f_{3x} \leq f_{max}$. Finally, the jamming avoidance formula $(-\mathbf{m}\cos\theta - \mathbf{n}\sin\theta) \cdot \mathbf{f} \geq 0$ generates the three constraints (7) $f_{1y}\cos\theta + f_{1z}\sin\theta \geq 0$, (8) $f_{2x}\sin\theta + f_{2y}\cos\theta \geq 0$, and (9) $-f_{3x}\sin\theta + f_{3z}\cos\theta \geq 0$.

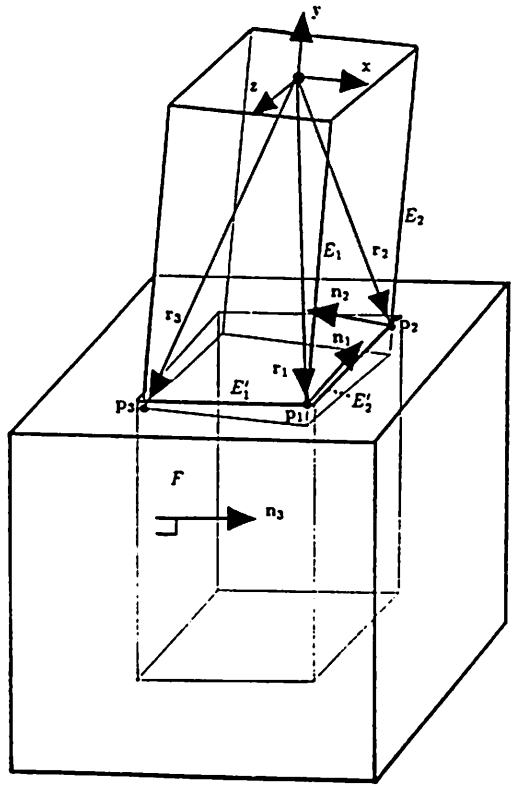

Figure 4. A 3-point contact state in a rectangular peg-in-hole insertion

When expressed in $f_1 \times f_2 \times f_3$-space with the single "$\leq$" relation, constaints (1)-(9) become:

$$\begin{pmatrix} 0 & 0 & 1 & 0 & 0 & 0 & 0 & 0 & 0 \\ 0 & 0 & 0 & 1 & 0 & 0 & 0 & 0 & 0 \\ 0 & 0 & 0 & 0 & 0 & 0 & -1 & 0 & 0 \\ 0 & 0 & -1 & 0 & 0 & 0 & 0 & 0 & 0 \\ 0 & 0 & 0 & -1 & 0 & 0 & 0 & 0 & 0 \\ 0 & 0 & 0 & 0 & 0 & 0 & 1 & 0 & 0 \\ 0 & -\cos\theta & -\sin\theta & 0 & 0 & 0 & 0 & 0 & 0 \\ 0 & 0 & 0 & -\sin\theta & -\cos\theta & 0 & 0 & 0 & 0 \\ 0 & 0 & 0 & 0 & 0 & 0 & \sin\theta & -\cos\theta & 0 \end{pmatrix} \begin{pmatrix} f_{1x} \\ f_{1y} \\ f_{1z} \\ f_{2x} \\ f_{2y} \\ f_{2z} \\ f_{3x} \\ f_{3y} \\ f_{3z} \end{pmatrix} \leq \begin{pmatrix} -f_{min} \\ -f_{min} \\ -f_{min} \\ f_{max} \\ f_{max} \\ f_{max} \\ 0 \\ 0 \\ 0 \end{pmatrix}$$

(5)

A matrix quasistatically relating the three contact forces to the applied wrench exerted through the insertor frame is constructed using the displacements r_1, r_2, and r_3 from the peg's coordinate frame origin to the respective points of contact P_1,P_2, and P_3 (refer to figure 4). From the object model,

$$r_1 = \begin{pmatrix} -1 \\ -4 \\ 1 \end{pmatrix}, \; r_2 = \begin{pmatrix} 1 \\ -4 \\ 1 \end{pmatrix}, \; r_3 = \begin{pmatrix} 1 \\ -4 \\ -1 \end{pmatrix}$$

so the projection matrix in equation (4) becomes

$$A = \begin{pmatrix} -1 & 0 & 0 & -1 & 0 & 0 & -1 & 0 & 0 \\ 0 & -1 & 0 & 0 & -1 & 0 & 0 & -1 & 0 \\ 0 & 0 & -1 & 0 & 0 & -1 & 0 & 0 & -1 \\ 0 & 1 & 4 & 0 & -1 & 4 & 0 & 1 & 4 \\ -1 & 0 & 1 & 1 & 0 & 1 & -1 & 0 & -1 \\ -4 & -1 & 0 & -4 & -1 & 0 & -4 & 1 & 0 \end{pmatrix}$$

A POP-11 implementation of the projection technique presented in section 3 was applied to the intersection of contact force halfspaces respresented by the nine inequalities of (5), using the above projection matrix A. The

halfspace intersection volume in 9-dimensional $f_1 \times f_2 \times f_3$-space has 9 hyperplanar facets of dimensionality 8, represented by the 9 inequalities. To obtain candidate hyperplanar faces of dimensinality 5 in 6-dimensional applied force space, the program computes the intersection of each 4-tuple of 8-dimensional surfaces. Out of a total of $\frac{9!}{4!(9-4)!} = 126$ 4-tuples, 66 of them yield 5-dimensional facets of the halfspace intersection volume (the other 60 4-tuples have nonindependent surface normals). Of these 66 facets, 12 project to boundary facets of the intersection volume's projection in applied force space. Of the 12 boundary facets, only two are distinct:

$$\begin{pmatrix} -0.9428 & 0.2357 & 0.0 & 0.0 & 0.0 & -0.2357 \\ 0.6860 & 0.0 & 0.6860 & -0.1715 & 0.0 & 0.1715 \end{pmatrix} \begin{pmatrix} F_x \\ F_y \\ F_z \\ M_x \\ M_y \\ M_z \end{pmatrix} \leq \begin{pmatrix} 0.0 \\ 0.0 \end{pmatrix}$$

As a necessary condition for satisfying all 9 contact force constraints, and a sufficient condition for satisfying at least one (see section 4), the robot must exert an applied wrench $(F_x, F_y, F_z, M_x, M_y, M_z)$ through the insertor's coordinate frame that satisfies the above two inequalities, whenever the insertor's configuration is near the nominal pose of the 3-point contact state shown in figure 4.

6 Discussion

For a robotic insertion task to succeed without interruption, the wrench that the robot exerts through the insertor's coordinate frame at any point along the trajectory must be chosen to avoid failure modes such as jamming and excess contact strain. The algorithm presented in section 3 provides a means for computing a set of constraint inequalities on the wrench which is applied to the insertor when it is in a multiple point-contact configuration relative

to the stationary container. If three or more contacts are involved, the constraints provide necessary, but not sufficient, conditions for a successful insertion. When sufficient conditions for a successful insertion cannot be derived, an error-recovery strategy may be required.

In our CAD-based approach to assembly task planning [3][5][9], a nominal assembly trajectory is first calculated from the symmetries of the parts, without the consideration of trajectory uncertainty and geometric tolerances. Sensor and control error are not considered in this phase, and the insertor and container are modelled for a perfect assembly involving zero clearance between their surfaces. Once a nominal trajectory is calculated, a compliant control strategy is synthesized to accommodate the contact states that could occur as the insertor traverses an uncertain trajectory.

The number of potential contact states that must be accommodated by the compliant control strategy may be reduced by imposing a desired sequence of contact states, as suggested by Caine [1]. When the number of anticipated contact states is reduced, the jamming-avoidance constraints are fewer in number, making it easier to find an applied wrench that may satisfy all of the local reaction force constraints [2]. A contact state sequence which involves a progressively increasing number of contacts may be enforced by using the breaking-contact constraints [1].

Applied force constraints are calculated at discrete configurations along the insertor's trajectory relative to the container. Configurations at which the two parts' set of contacting surface features changes (assuming zero-clearance between the parts) provide us with *critical points* in the trajectory, i.e., nominal configurations where failure modes can occur. At each critical point, small perturbations in the insertor's configuration can give rise to several possible combinations of contacting surface features. The possible contact combinations that may occur are determined through a linear programming technique, involving the detection of nonempty intersections of

linearized C-surface patches.

Each possible combination of contact forces has an associated quasi-static relationship to the wrench exerted through the insertor frame. Using the quasi-statics matrix formulated in equation (4) of section 5, contact force constraints to prevent jamming, breaking of contact, and excess strain may be projected to applied wrench space. The resulting wrench constraints are necessary, but not sufficient, conditions for avoiding these failure modes. Applied wrench constraints computed for a given combination of contacts are merged with constraints arising from the other contact combinations anticipated at the critical point, delimitting the applied wrenches that should be commanded at that point in the trajectory.

Recall from section 3 that the algorithm for projecting a volume consisting of the intersection of m_1 linear constraints in $\Re^{n_1}$ into $\Re^{n_2}$ involves the processing of $\frac{m_1!}{k!(m_1-k)!}$ k-tuples of linear constraints, where $k = n_1 - n_2 + 1$. The computational cost of projecting contact force constraints into applied wrench space is heavily dependent on the number of contacts involved and the number of constraints per contact. If we impose m reaction force constraints per contact, then each combination of n simultaneous contacts provides a set of $m_1 = mn$ contact force constraints in $\Re^n_1 = \Re^{3n}$. For 3-dimensional insertions, $n_2 = 6$, the dimensionality of wrench space.

When m and n are small, the projection algorithm provides a fairly tractable means for projecting mn constraints from $\Re^{3n}$ into $\Re^6$. But due in part to the number $\frac{m_1!}{k!(m_1-k)!}$ of k-tuples of constraints to be processed, the algorithm blows up rapidly as m and n increase. The following table shows the number of k-tuples of linear constraints that must be processed in the projection operation, as a function of m and n (cases where there are not enough contact force constraints to form k-tuples, or the wrench space is of higher dimension than the contact force space are omitted).

	n				
m	$\frac{m_1!}{k!(m_1-k)!}$	2	3	4	5
	1	2	*	*	*
	2	4	15	8	1
	3	6	126	792	3003
	4	8	495	11440	184756

The projection algorithm has been implemented in POP-11 running on a Sun 3 workstation. The rectangular peg-in-hole example in section 5, which involves $m = 3$ failure modes and $n = 3$ contact forces required somewhat more than a minute of runtime to process the 126 k-tuples of reaction force constraints.

7 Conclusion

An algorithm was presented for projecting the intersection of m linear half-spaces in $\Re^n$ into a lower-dimensional subspace of $\Re^n$. We demonstrated how this algorithm may serve as a tool in developing compliant control strategies for insertion tasks. The prohibition of failure modes such as jamming and excess strain may be represented by linear inequality constraints delimitting a volume in contact force space. Using the algorithm described in section 3, this volume may be projected into applied wrench space, yielding a bounded set of wrenches that the robot may exert through the insertor's coordinate frame. The projection algorithm, which is computationally practical for reasonably small numbers of point contacts and failure modes, effectively automates the manual force constraint derivation approach of Whitney [11]. However, we proved in section 4 that if the applied wrench space is of lower dimension than the space of contact force components, as is the case in Whitney's derivation, the resulting applied wrench constraints provide only necessary, not sufficient, conditions for avoiding failure modes such as jamming.

8 References

1. Caine, M.E. (1985), "Chamferless Assembly of Rectangular Parts in Two and Three Dimensions", S.M. Thesis, Department of Mechanical Engineering, Massachusetts Institute of Technology.

2. Caine, M.E., Losano-Perez, T., Seering, W.P. (1989), "Assembly strategies for chamferless parts", *Proceedings of the IEEE International Conference on Robotics and Automation*, pp. 472-477.

3. Dakin, G., Liu, Y., Nair, S., Popplestone, R.J., Weiss, R. (1989), "Symmetry inference in planning assembly", *Proceedings of the IEEE International Conference on Robotics and Automation*, Vol. 3, pp. 1865-1868.

4. Johnson, L.W., Riess, R.D. (1981), *Introduction to Linear Algebra*, Reading, Mass.: Addison-Wesley Publishing Company.

5. Liu, Y. (1989), "Planning for assembly from solid models", *Proceedings of the IEEE International Conference on Robotics and Automation*, pp. 222-227.

6. Ohwovoriole, M.S., Hill, J.W., Roth, B.(1980), "On the theory of single and multiple insertions in industrial assemlies", *Proceedings of the 10th International Symposium on Industrial Robots*, Milan, Italy, March 1980, pp. 545-558.

7. Ohwovoriole, M.S., Roth, B.(1981), A theory of parts mating for assembly automation", *Proceedings of the Robot and Man Symposium 81*, Warsaw, Poland, Sept. 1981.

8. Popplestone, Ambler, A.P., Bellos, I. (1980), "An interpreter for a language describing assemblies", Artificial Intelligence, Vol. 14, No. 1, pp.

79-107.

9. Popplestone, R., Grupen, R., Liu, Y., Dakin, G., Oskard, D. Nair, S. (1989), "Planning for assembly with robot hands", *SPIE Advances in Intelligent Robotics / Visual Communications and Image Processing*, Philadelphia, Pa. Nov. 5-10, 1989, by invitation.

10. Simunovic, S. (1975), "Force information in assembly processes", *Proceedings of the 5th International Symposium on Industrial Robotics*, pp. 415-427.

11. Whitney, D.E. (1982), "Quasi-static assembly of compliantly supported rigid parts", *Journal of Dynamic Systems, Measurement, and Control*, Vol. 104, pp. 64-77.